Trade-offs Between Discretization Approaches in Urban Stormwater Modeling: Accuracy, Interpretability, and Practical Implications

Zhaokai Dong[a*], Sabrina Jivani[a], Pradeep Goel[b], and Clare E. Robinson[a]

[a] Department of Civil and Environmental Engineering, Spencer Engineering Building, Western University, 1151 Richmond St, London, ON N6A 3K7, Canada.

[b] Water Monitoring Section, Environmental Monitoring and Reporting Branch, Ministry of the Environment, Conservation and Parks, 125 Resources Road Etobicoke, ON, M9P3V6, Canada.

*Corresponding author email: zdong262@uwo.ca

1   **Abstract**

2   Stormwater models are important tools for urban drainage design, planning, and analysis, but

3   their performance and interpretation depend heavily on how spatial discretization is handled.

4   This study evaluates the influence of two common discretization strategies – topography- and

5   sewer geometry-based – on hydrological representation and simulation accuracy in the Storm

6   Water Management Model (SWMM), using a mixed urban and peri-urban watershed in London,

7   ON, Canada. Leveraging long-term flow data from multiple monitoring locations across the

8   watershed, we systematically evaluated the effects of discretization strategy across different

9   rainfall conditions and land use settings (e.g., urban vs. peri-urban) using continuous and event-

10   based simulations, as well as a fixed-effects regression model. The two models with different

11   discretization approaches showed no significant differences in simulating outlet flows, indicating

12   that discretization choice had limited impact on outlet flow simulations. However, the

13   topography-based model yielded parameter values with greater hydrological interpretability and,

14   accordingly, performed better at simulating flows at locations within the watershed. In addition,

15   model performance was strongly influenced by rainfall depth and land use characteristics, with

16   significantly improved results observed during larger storm events and in the urban watershed.

17   The strengths and limitations of the two discretization approaches are laid out based on the study

18   findings. Ultimately, the study demonstrates that discretization choice can significantly influence

19   model structure, parameter interpretation, and spatial simulation accuracy, particularly in

20   watersheds with heterogeneous topography and mixed drainage systems, and should therefore be

21   carefully considered in stormwater modeling and scenario planning.

22 **Keywords**

23 Stormwater modeling; spatial discretization; hydrological representation; performance; urban

24 and peri-urban watersheds

1. Introduction

Urban stormwater management is a major challenge as urbanization increases impervious surface cover, resulting in higher stormwater flow volumes and peak flow rates (Hopkins et al., 2014; Jefferson et al., 2017). To support stormwater regulation and planning, hydrologic-hydraulic stormwater models – such as the U.S. EPA Storm Water Management Model (SWMM) – are widely used to simulate flow responses of urban drainage systems to precipitation events (Niazi et al., 2017). These models help planners and practitioners assess existing drainage infrastructure networks, evaluate and design stormwater control measures, and evaluate alternative land use scenarios.

Spatial discretization of the watershed is an essential step in constructing stormwater models whereby the boundaries of subcatchments (fundamental drainage areas) that direct local runoff to sewer systems are determined (Rossman and Huber, 2016). In urban settings, this task is challenging as runoff pathways are influenced by both the engineered drainage infrastructure (e.g., sewer inlets and pipes) and complex human-modified surface topography (Gironás et al., 2010; Dong et al., 2022). At high spatial resolution, small urban parcels (e.g., buildings) can be modeled as individual subcatchments, routing overland flow to a nearby sewer inlet, which closely reflects actual drainage behavior. While effective at the block scale, such fine-scale mapping is time-intensive and often not practical for larger watersheds or scenario-based planning (Dong et al., 2022; Si et al., 2024). Hence, model discretization approaches that can provide physically based representation of stormwater drainage behavior but with reduced spatial complexity are favored for larger-scale models (greater than a few blocks) (Dobson et al., 2022).

46   Two simplification strategies are commonly used for discretization of large watersheds, each

47   with distinct strengths and limitations. The first is a topography-based approach, which uses

48   digital elevation models (DEMs) to determine subcatchment boundaries and outlets. Since

49   subsurface drainage infrastructure is not represented in DEMs, sewer network data is often

50   integrated with the subcatchment delineation to manually define surface-subsurface flow paths

51   (i.e., connecting subcatchment outlets to sewer inlets). Additional adjustments can be made

52   during this process to refine the initial DEM-based delineations (Si et al., 2024). To improve

53   efficiency, "burning" techniques have also been used to improve representation of engineered

54   drainage pathways by lowering DEM elevations along known sewer alignments such as sewer

55   inlets or pipes (Gironás et al., 2010; Si et al., 2024; Sokolovskaya et al., 2023). Yet, variations in

56   DEM resolution and data processing steps may introduce variability in discretization outcomes,

57   resulting in inconsistent estimations of subcatchment characteristics and, ultimately, affecting

58   simulation results (Gironás et al., 2010).

59   The second strategy is a sewer geometry-based approach, where subcatchments are discretized

60   by drawing Thiessen polygons around the sewer inlets. This method directs surface runoff within

61   each polygon to its nearest inlet, thereby simplifying the physical definition of drainage

62   boundaries and their connection to the sewer system. Recently, the sewer geometry-based

63   approach has gained popularity due to its ease of use and efficient integration with available

64   infrastructure datasets (Dong et al., 2022; Li et al., 2024; Ni et al., 2025; Qi et al., 2025). Studies

65   have shown that this approach can provide reliable pipe flow predictions at the outlet of urban

66   watersheds (Dong et al., 2022). However, the lack of consideration for topographic

67   characteristics may result in less accurate representation of terrain-driven flow patterns, such as

68   runoff along roads to drains. This limitation may reduce the accuracy of the model in simulating

69   flow accumulation within the watershed, potentially leading to misclassification of areas

70   vulnerable to localized flooding.

71   Although prior studies have qualitatively examined the influence of the two approaches on

72   simulating stormwater flows through scenario testing using uncalibrated SWMM models (Dong

73   et al., 2022; Li et al., 2024), there remains limited understanding of how choice of discretization

74   strategy affects model structure, calibration, parameter interpretation, and performance under

75   varying rainfall and land use conditions. This question is particularly relevant for simulating

76   alternative stormwater management scenarios, where model outputs are used to inform decision-

77   making. If choice of discretization strategy introduces additional model uncertainty, simulation

78   results may provide biased guidance when comparing different management alternatives. In

79   addition, while stormwater runoff collection and conveyance in highly urbanized areas typically

80   rely on engineered drainage infrastructure (e.g., sewer systems), engineered drainage networks in

81   urban-rural transitional areas (i.e., peri-urban) are often incomplete (Niazi et al., 2017). As a

82   result, peri-urban areas usually have a combination of fast and slow hydrological responses to

83   storm events (Braud et al., 2013). Considering the different drainage systems between urban and

84   peri-urban watersheds, different discretization methods may yield distinct representations of

85   dominant drainage processes, potentially making one approach more suitable than another

86   depending on watershed drainage and land use characteristics. However, this hypothesis has not

87   been evaluated previously. With urban areas rapidly expanding globally, understanding the

88   influence of spatial discretization choices on model performance, across watersheds with

89   different degrees of urbanization, is needed to develop effective and reliable stormwater models,

90   and in turn support informed stormwater planning and design.

91   The objective of this study is to evaluate and compare the performance, sensitivity, and

92   interpretability of stormwater models developed using topography- and sewer geometry-based

93   discretization approaches. To address this, we develop two SWMM models of a highly

94   monitored watershed in London, Canada using topography-based and sewer geometry-based

95   discretization approaches. Using continuous and event-based simulations, along with fixed-

96   effects regression, we evaluate how discretization strategy affects model performance across

97   different land use types, storm event sizes, and monitoring locations at the outlets and within the

98   watershed. This quantitative comparison is used to clarify the tradeoffs in selecting a

99   discretization strategy including model physical realism, simplicity of implementation, and

100   model performance. Overall, this study provides new insights to support discretization strategy

101   selection for efficient, reliable stormwater scenario simulations.

102   **2. Methods**

103   **2.1 Study site and data**

104   The study area is the Thornicroft Drain watershed, located in London, ON, Canada (Figure 1A

105   and Figure S1 Supplementary Material (SM)). The watershed area is approximately 580 ha. The

106   upper watershed (~210 ha) is highly urbanized, with 94% of the area consisting of urban land

107   uses, including residential, commercial, industrial, and transportation. Stormwater runoff is

108   collected and conveyed through a separated sewer system and discharged to the Thornicroft

109   Drain open channel at the upper outlet. The lower watershed (~370 ha) is a peri-urban area

110   comprising 50% rural land uses, including agricultural land and forest. Most stormwater runoff

111   in the lower watershed drains directly to Thornicroft Drain, except for one residential

112   neighborhood (~100 ha) that is serviced by a separated sewer system that ultimately discharges

113   into Thornicroft Drain. The primary soil type in urban land use areas is silty clay, while silty

114   sand is the primary soil type in rural land use areas. Hereafter, we refer to the upper watershed as

115   the upper urban watershed and the lower watershed as the lower peri-urban watershed, based on

116   their distinct land use characteristics and stormwater drainage infrastructure.

117
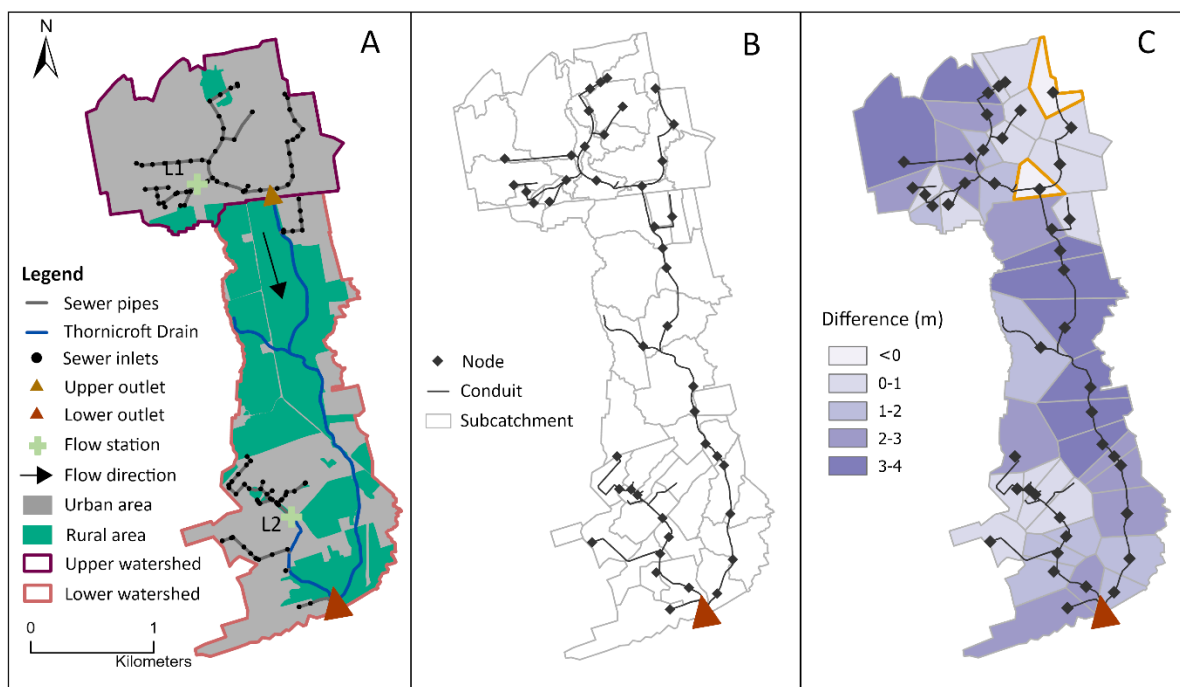
118   **Figure 1.** (A) major land use within upper watershed and lower watershed areas, stormwater

119   drainage pathways, and flow monitoring stations at the outlets of the upper and lower watersheds

120   and at two locations within the watershed (L1 and L2). Model configurations developed based on

121   (B) topography-based discretization and (C) sewer geometry-based discretization. Elevation

122   difference between subcatchment average elevation and corresponding node elevation for sewer

123   geometry-based discretization model is shown in panel (C). Subcatchments for which the

124   average surface elevation is less than the node elevation are marked with orange border.

125　Stormwater flow monitoring was conducted from August 2021 to November 2023 at the outlets

126　of the upper urban watershed and the lower peri-urban watershed. At these locations water levels

127　in Thornicroft Drain were continuously measured at 15-minute intervals using a pressure

128　transducer (TD/CTD Diver, Van Essen Instruments). Measured water levels were converted to

129　flow rates by developing rating curves for each location. These rating curves were based on flow

130　rate measurements performed using a portable flow meter (HACH FH950) across a wide range

131　of flow conditions. Over the same monitoring period, flows were also measured at two locations

132　within the watershed – L1 (a storm drain) within the upper urban watershed and L2 (an open

133　drain) within the lower peri-urban watershed. Further details of the monitoring program and

134　dataset are available in Vyn (2023). As snowmelt data during the monitoring period are not

135　available, this study focuses on simulating stormwater flows during the warm season (June to

136　October).

137　Rainfall data with 5-minute resolution were obtained from two City of London rain gauges

138　located 0.6 km southwest and 1.7 km northeast of the watershed boundary (Figure S1). Sewer

139　infrastructure data, including spatial layout and pipe geometry, were provided by the City of

140　London. Spatial datasets were obtained from the Ontario Ministry of Natural Resources and

141　Forestry (OMNRF, 2019), including a 2-m LiDAR-derived digital elevation model (DEM) and

142　0.5-m resolution aerial imagery. Daily climate data, including minimum and maximum

143　temperatures, were collected from Environment and Climate Change Canada (EMCC, 2024). A

144　summary of all datasets used in this study is provided in SM Table S1.

2.2 Model development

145

146 The U.S. EPA Storm Water Management Model (SWMM) was used to simulate stormwater

147 flows in the study watershed. SWMM is a widely used for urban stormwater simulations

148 (Rossman and Huber, 2016). It simulates runoff generation from subcatchments (the basic

149 hydrological units) and routes the resulting flow through sewer networks to an outfall. Watershed

150 discretization, a fundamental step in model development, involves delineating subcatchment

151 boundaries and specifying the direction of stormwater runoff toward sewer inlets. In this study,

152 two SWMM models were developed using the same precipitation input and sewer data (Table

153 S1), but with the watershed discretized using topography- and sewer geometry-based methods,

154 respectively.

155 For the topography-based model, subcatchment boundaries were delineated using ArcGIS

156 hydrologic analysis tools applied to raw DEM data. These included sink filling, flow direction

157 and accumulation, and watershed basin delineation (Bibi, 2022). In urban areas, the resulting

158 subcatchments were overlaid with sewer network data to refine boundaries and assign

159 subcatchment outlets to sewer inlets, with additional expert input from City of London

160 stormwater engineers. For subcatchments without nearby sewer infrastructure, stormwater runoff

161 was routed to adjacent downstream subcatchments or directly to Thornicroft Drain.

162 In the sewer geometry-based model, watershed discretization was completed by drawing

163 Thiessen polygons around nodes (e.g., sewer inlets), such that any point within a polygon is

164 closer to its corresponding node than to any other node (i.e., representing the shortest flow path).

165 This approach assumes that each node is located at a minimum local elevation, allowing runoff

166 from the surrounding area to be routed to that node (Dong et al., 2022). Although Dong et al.

9

167   (2022) showed that the location of nodes used to generate polygons does not significantly impact

168   outlet flow simulations, identical node locations were used in both the topography-based and

169   sewer geometry-based models to ensure consistent comparisons of inflows at each node.

170   Specifically, subcatchment outlets from the topography-based model were used to generate

171   polygons.

172   The slope and imperviousness parameters for each subcatchment were first determined using

173   DEM data and aerial imagery (Figure S2). As SWMM assumes spatial-uniform characteristics

174   within each subcatchment, area-weighted averages were assigned to each subcatchment.

175   Subcatchment width, representing the stormwater overland flow width, was inferred from spatial

176   data. In the topography-based model, the subcatchment width was initially calculated by dividing

177   the subcatchment area by the flow path length determined from the DEM, with outlets typically

178   located at the downslope edge of the subcatchment (Figure S2A). In the sewer geometry-based

179   model, subcatchment width was estimated by dividing the subcatchment area by a two-sided

180   symmetrical flow length (Rossman and Huber, 2016). The one-side flow length (i.e., half of the

181   two-sided symmetrical length) was calculated as the longest distance from any point within the

182   subcatchment to its corresponding sewer inlet (Dong et al., 2022).

183   Other parameters that cannot be derived using spatial data were obtained from literature,

184   including Manning's roughness, depression storage, and pipe roughness (Behrouz et al., 2020;

185   Bisht et al., 2016; Dong et al., 2022; Krebs et al., 2014; Lee et al., 2018; Macro et al., 2019;

186   Perin et al., 2020; Wu et al., 2024; Zhuang et al., 2023). In both models, infiltration was

187   simulated using the Green-Ampt method, which requires specification of soil parameters

188   including saturated hydraulic conductivity, suction head, and initial moisture deficit. Subsurface

189   flow was simulated using the SWMM groundwater module, which represents surface runoff-

190   groundwater interactions by simulating water movement between an upper unsaturated soil zone

191   and a lower saturated soil zone. Parameters estimated for this module include aquifer porosity,

192   field capacity, and saturated hydraulic conductivity. Parameter values related to infiltration and

193   groundwater modules were adopted from a previous study by Jivani (2024), who calibrated these

194   parameters using flow data measured within the watershed. Further information on estimation of

195   these parameters and values used is provided in Table S2.

2.3 Model calibration and evaluation

197   Model calibration was performed using continuous flow data from August to October 2021.

198   Given the distinct land use characteristics between the upper and lower watersheds, the

199   parameters for subcatchments in the upper urban watershed were first calibrated using the upper

200   outlet flow data. Following this, the parameters for subcatchments in the lower peri-urban

201   watershed were calibrated using lower outlet flow data, while keeping the parameters calibrated

202   for the upper subcatchments fixed. This stepwise calibration helped reduce the influence of

203   parameterization in the upper watershed on simulations in the lower watershed. Parameters for

204   calibration included subcatchment width, Manning's roughness, depression storage, and pipe

205   roughness. The Nash-Sutcliffe Efficiency (NSE, Equation 1) (Nash and Sutcliffe, 1970) was

206   used as the primary performance evaluation metric (both for calibration and validation), with this

207   metric supplemented by runoff volume error (Equation 2), peak flow error (Equation 3), and

208   time-to-peak error (Equation 4), and flow residuals (Equation 5).

209   $\text{NSE} = 1 - \frac{\sum_{i=1}^{n}(Q_{o,i} - Q_{s,i})^2}{\sum_{i=1}^{n}(Q_{o,i} - \overline{Q_O})^2}$ Equation 1

210   $\text{Volume error} = \frac{\sum_{i=1}^{n}(Q_{o,i} - Q_{s,i})}{\sum_{i=1}^{n}(Q_{o,i})} \times 100\%$ Equation 2

211   Peak flow error $= \frac{(P_{o,i} - P_{s,i})}{P_{o,i}} \times 100\%$ Equation 3

212   Time-to-peak error $= (t_{o,i} - t_{s,i})$ Equation 4

213   Flow residual $= Q_{s,i} - Q_{o,i}$ Equation 5

214   where $Q_{o,i}$ and $Q_{s,i}$ are the observed and simulated flow rates (m³/s), respectively, $\overline{Q_O}$ is the

215   observed mean flow (m³/s); $P_{o,i}$ and $P_{s,i}$ are the observed and simulated peak flow rates (m³/s),

216   respectively, and $t_{o,i}$ and $t_{s,i}$ are the time corresponding to the observed and simulated peak flow

217   rates (min), respectively. An NSE value closer to 1 indicates better model performance.

218   Validation was conducted using continuous flow data from June to October for 2022 and 2023 at

219   the upper and lower watershed outlets, along with two monitoring locations that are within the

220   upper urban watershed (L1) and lower peri-urban watershed (L2), receptively (flow data from

221   2021-2023). In addition to calibrating and validating the model based on continuous flow

222   simulations, model performance was also evaluated at the event scale. For this, continuous data

223   were divided into individual storm events using a 6-hour inter-event dry period (Dong et al.,

224   2024a). The same performance metrics used for the continuous flow models were applied to

225   evaluate the performance of the event-based models.

226   To assess the influence of discretization method on the performance of the models across

227   different rainfall depths and land use characteristics (urban versus peri-urban), a linear fixed-

228   effects model was applied. This statistical approach evaluates how specific factors affect an

229   outcome (i.e., response variable; Equation 6) (John Fox, 2015).

230    $y_i = \sum \beta_j \cdot x_{i,j} + \alpha_j + \varepsilon_{i,j}$ Equation 6

231   here β_j is a coefficient describing the influence of the jth predictor $x_{i,j}$ on performance metric

232   y_i in the ith event, α_j is the unobserved event-invariant effect (e.g., the distinct effects of upper

233   and lower watershed land uses) $\varepsilon_{i,j}$ is a stochastic error term with an expected value of zero

234      $E[\varepsilon_{i,j}] = 0$, and constant variance $E[\varepsilon_{ij}^2] = \sigma^2$.

235   Model performance metrics, including NSE, peak error, volume error, and time-to-peak error,

236   were used as response variables (y_i). Discretization method, rainfall depth, and watershed land

237   use characteristics were treated as fixed effects (predictors) to test whether variations in model

238   performance could be attributed to these factors. Events with rainfall depths less than 1 mm were

239   excluded to reduce noise from low-intensity events that do not generate runoff. Categorical

240   predictors were modeled as binary: sewer-based discretization and lower outlet were assigned as

241   0, while topography-based discretization and upper outlet were assigned as 1.

242   Finally, to assess the hydrological interpretability of parameter values, Spearman's correlation

243   analysis was used to examine the relationships between discretization-related parameters

244   (including imperviousness, slope, drainage area, and width) and subcatchment outputs (e.g.,

245   runoff volume and peak runoff rate) across all subcatchments. The physical interpretability of the

246   discretization-related parameters was evaluated through correlation strength, with stronger

247   correlations indicating greater physical relevance.

248   **3. Results and Discussion**

249   **3.1 Model configurations**

250   Model configurations derived from the two discretization approaches are shown in Figure 1B-C.

251   The sewer geometry-based model comprised 44 subcatchments, with 19 of these subcatchments

252 located in the upper urban watershed. All subcatchments except two have average elevations

253 higher than their outlet node elevations (Figure 1C). The two subcatchments with average

254 elevations slightly lower than those of their corresponding outlet nodes had elevation differences

255 less than 0.1%. This suggests the "naive" surface-to-node flow assumption (i.e., routing runoff

256 toward the nearest node) is generally acceptable, as this modest elevation difference could result

257 from data processing processes or limitations in DEM resolution (Dong et al., 2022). This aligns

258 with the findings of Dong et al. (2022), who showed that most subcatchments in their modeled

259 sewershed satisfied the surface-to-node assumption. In comparison to the sewer geometry-based

260 model, the topography-based model has 52 subcatchments, including 22 in the upper urban

261 watershed. In the topography-based model, stormwater runoff from eight of the subcatchments

262 (three in the upper watershed) is routed to the adjacent downstream subcatchment, while runoff

263 in the remainder of the subcatchments is routed directly to a sewer inlet or Thornicroft Drain.

264 **3.2 Comparison of discretization-related parameters**

265 Figure 2 shows a comparison of the discretization-related subcatchment physical parameters

266 between the topography- and sewer geometry-based models. For both models, subcatchment

267 areas in the lower peri-urban watershed were generally larger than those in the upper urban

268 watershed. In the sewer geometry-based model, the area of the subcatchments varies from 3.1-

269 17.2 ha (mean = 11.6 ha) in the upper urban watershed and from 3.9-28.8 ha (mean =14.7 ha) in

270 the lower peri-urban watershed, while in the topography-based model, the area varies from 1.9-

271 28.7 ha (mean = 10.3 ha) in the upper watershed and from 3.1-29.9 ha (mean =13.4 ha) in the

272 lower watershed. In the sewer geometry-based model, the delineation resolution (shape) depends

273 on the spatial distribution of nodes (e.g., sewer inlets), resulting in finer subcatchments in the

274 upper watershed where nodes were more densely distributed. In contrast, topography-based

14

275　delineation was determined based on terrain variation and flow paths. In the upper urban

276　watershed, anthropogenic modifications to the terrain, such as road crowns and lot grading, could

277　alter natural flow paths, thereby producing relatively smaller drainage areas.

278
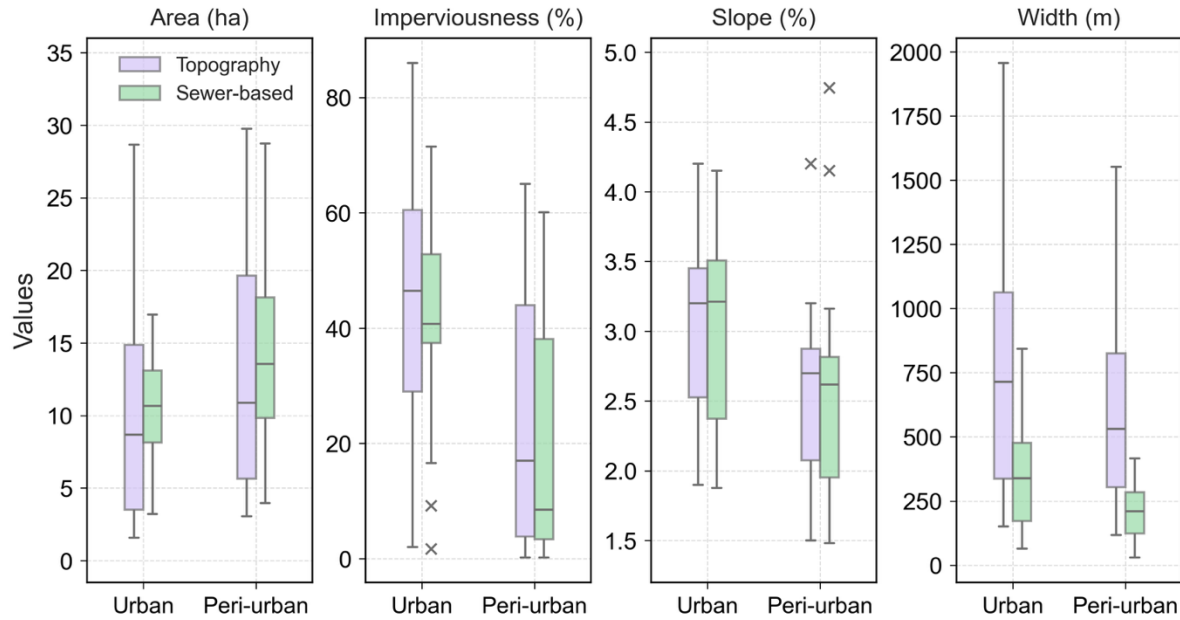
279　**Figure 2.** Comparison of discretization-related physical parameters (area, imperviousness, slope,

280　and width) for the subcatchments in the two models. The horizontal lines within the boxes show

281　the median value. The bottom and top of the box show the 25th and 75th quantiles. The whiskers

282　extend 1.5 times the interquartile range (IQR; 25th and 75th quantiles).

283　In the urban watershed, the subcatchments in the topography-based model had greater variability

284　in imperviousness compared to the sewer geometry-based model (Figure 2). This may be due to

285　the drainage areas (i.e., subcatchments) produced by the topography-based delineation

286　aggregating less heterogeneous land cover within individual subcatchments. In contrast, the

287　sewer geometry-based delineation, which does not account for topography, resulted in

288　subcatchments with more mixed land cover (varying degrees of imperviousness), ultimately

15

289   resulting in a narrower range of imperviousness. In the lower peri-urban watershed, the

290   imperviousness generated by the two models was comparable, likely due to the lower degree of

291   urbanization in the lower watershed. Subcatchment slopes showed limited difference between the

292   models, with both having steeper slopes in the upper watershed compared to the lower watershed

293   (Figure 2 and Figure S2C).

294   Subcatchment width, after calibration, varied considerably between the two models (Figure 2). In

295   general, the width values for subcatchments in the topography-based model were larger

296   compared to the sewer geometry-based model. This suggests that polygon-based subcatchments

297   created in the sewer geometry-based model tend to generate narrow overland flow paths (or

298   channels). Considering that the flow paths derived based on terrain variation in the topography-

299   based model aligned well with the road distributions (Figure S2A), topography-derived

300   subcatchment width may better reflect the actual overland flow width.

301   Correlation analysis showed that, in both the upper and lower watersheds, the topography-based

302   model exhibited stronger relationships between the discretization-related physical parameters

303   and subcatchment hydrological outputs (i.e., surface runoff volume and peak runoff rate) (Figure

304   3). While the strength of correlation between subcatchment parameter values and model outputs

305   does not directly influence model performance, it provides a useful means to assess whether

306   these parameters physically represent hydrological processes, based on current understanding of

307   their influence on runoff generation and flow dynamics. Two strong, positive correlations,

308   reflecting key input-output relationships, have been consistently observed and are well-

309   established: (1) between imperviousness and runoff volume, and (2) between subcatchment

310   width and peak flow (Behrouz et al., 2020; Dong et al., 2022). If model parameters are better

311   estimated in one model, we would expect stronger correlation strengths between these two input-

312   output pairs. Figure 3 shows that imperviousness was more strongly correlated with runoff

313   volume in the topography-based model (mean ρ across the upper and lower watersheds = 0.81)

314   than in the sewer geometry-based model (mean ρ = 0.61). Similarly, peak flow was more

315   strongly correlated with subcatchment width in the topography-based model (mean ρ = 0.71)

316   compared to the sewer geometry-based model (mean ρ = 0.39). These results indicate that the

317   parameter values from the topography-based model may have greater hydrological

318   interpretability. In addition, stronger inter-parameter correlations were observed in the

319   topography-based model. For instance, in the upper urban watershed, subcatchment area was

320   highly correlated with width in the topography-based model (ρ = 0.96), compared to a weaker

321   correlation in the sewer geometry-based model (ρ = 0.34). For an ideal discretization, minor

322   changes in drainage area boundaries should not substantially alter the estimation of actual flow

323   paths (e.g., runoff traveling along roads before entering a sewer inlet), although changes in the

324   boundaries may influence the volume of runoff entering the sewer inlet. The stronger correlation

325   strength between subcatchment area and width observed in the topography-based model suggests

326   that this discretization approach may produce more consistent estimates of flow path lengths.

327   Overall, the comparison of parameter values and the results of correlation analysis suggest that

328   the topography-based discretization approach may yield more physically meaningful parameter

329   values than the sewer geometry-based discretization approach.
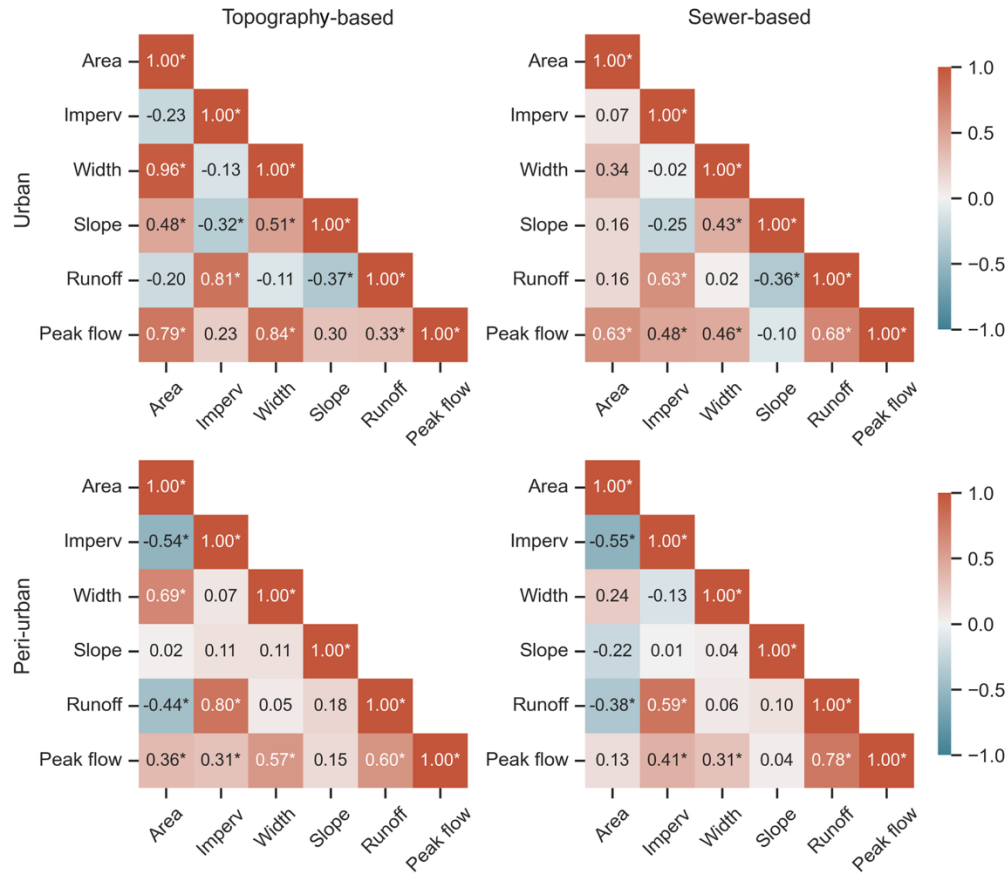
Figure 3. Spearman correlation coefficients across discretization-related subcatchment physical parameters (area, width, imperviousness, and slope) and model outcomes (subcatchment runoff volume, represented by runoff in the figure, and peak flow). An asterisk (*) indicates values with $p < 0.01$.

3.3 Model performance evaluation

3.2.1 Overall model performance

Model calibration and validation results are shown in Figure 4 and Table S3. Both models achieved high NSE values (> 0.9) during calibration using 2021 flow data at the lower and upper watershed outlets, indicating good agreement between simulated and observed flows. At the upper outlet, NSE values were 0.96 for the topography-based model and 0.93 for the sewer

341 geometry-based model. At the lower outlet, NSE values were 0.95 and 0.91, respectively.

342 Validation using 2022-2023 data suggests slightly reduced model performance for both models,

343 but the simulated flows still matched well with the observations, with all NSE values > 0.8

344 except for the sewer geometry-based model at the lower outlet in 2022 (0.64). In addition, at the

345 upper outlet, the topography-based model produced smaller absolute runoff volume errors (-

346 6.5% and -13.2% for 2022 and 2023, respectively) and peak flow errors (2.6% and -8.1%)

347 compared to the sewer geometry-based model, which had volume errors of -28.1% and -22.6%,

348 and peak flow errors of 2.6% and -19.5% for 2022 and 2023, respectively (Table S3 and Figure

349 S3). Similar differences in runoff volume and peak flow errors between the models were

350 observed at the lower outlet, except in 2023, when the absolute runoff volume error for the

351 topography-based model (25.1%) was higher than that of the sewer geometry-based model (-

352 8.1%).

353
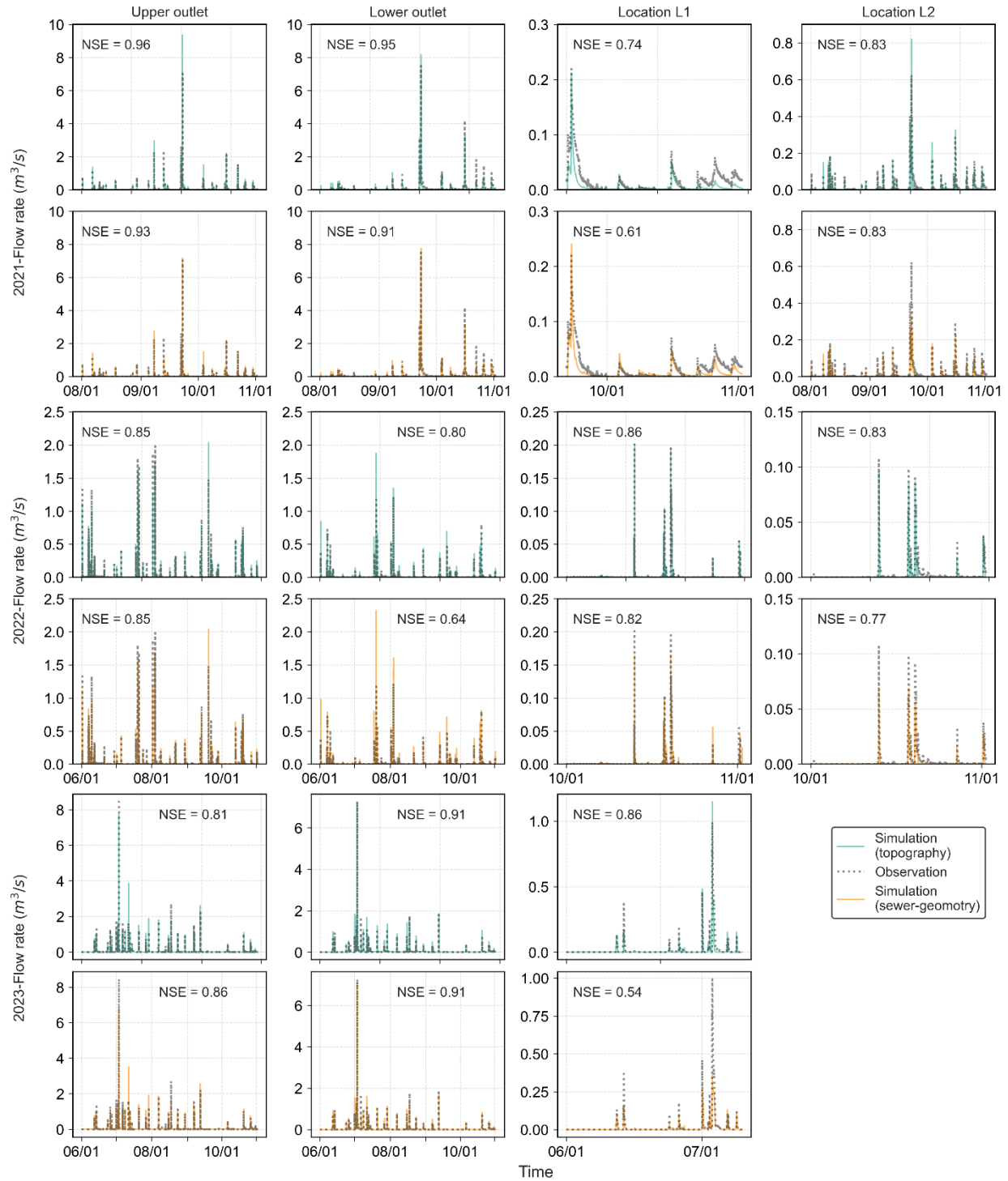
Figure 4. Simulation results at the upper and lower outlets and at the two flow monitoring locations within the upper (L1) and lower (L2) watersheds. Data from 2021 at the two outlets were used for model calibration, while the remaining data were used for model validation.

20

357 Flow residuals at the upper outlet from the two models were similar and tightly clustered around

358 the 1:1 line ($R^2 = 0.92$, Figure 5A). These results suggest that the discretization approach used

359 had limited influence on error structure at the outlet of the urban watershed. In contrast, residuals

360 between the two models diverged substantially at the lower outlet ($R^2 = 0.48$, Figure 5B). This

361 indicates increased sensitivity to discretization approach used in peri-urban areas. In addition, for

362 both models, residuals decreased as rainfall intensity increased (Figure 5C-D). This may be

363 because infiltration, evapotranspiration, and groundwater processes become more important for

364 smaller rainfall events particularly in the peri-urban area and it is possible that these processes

365 may be less accurately represented (Dong et al., 2024b; Irvine et al., 2024; Vrugt et al., 2024).

366 The lower model performance for the 2022 validation period could therefore be due to the

367 relatively dry weather and the resulting low-flow conditions during that year. These findings

368 indicate that the faster, simpler sewer geometry-based discretization approach may be sufficient

369 for simulating outlet flows in urban watersheds. However, in peri-urban areas with more

370 complex, terrain-driven runoff pathways, even though both models were able to capture the

371 observed overall flow processes at the lower outlet, the topography-based model generally

372 performed better than the sewer geometry-based model, as indicated by its relatively higher NSE

373 values.

374
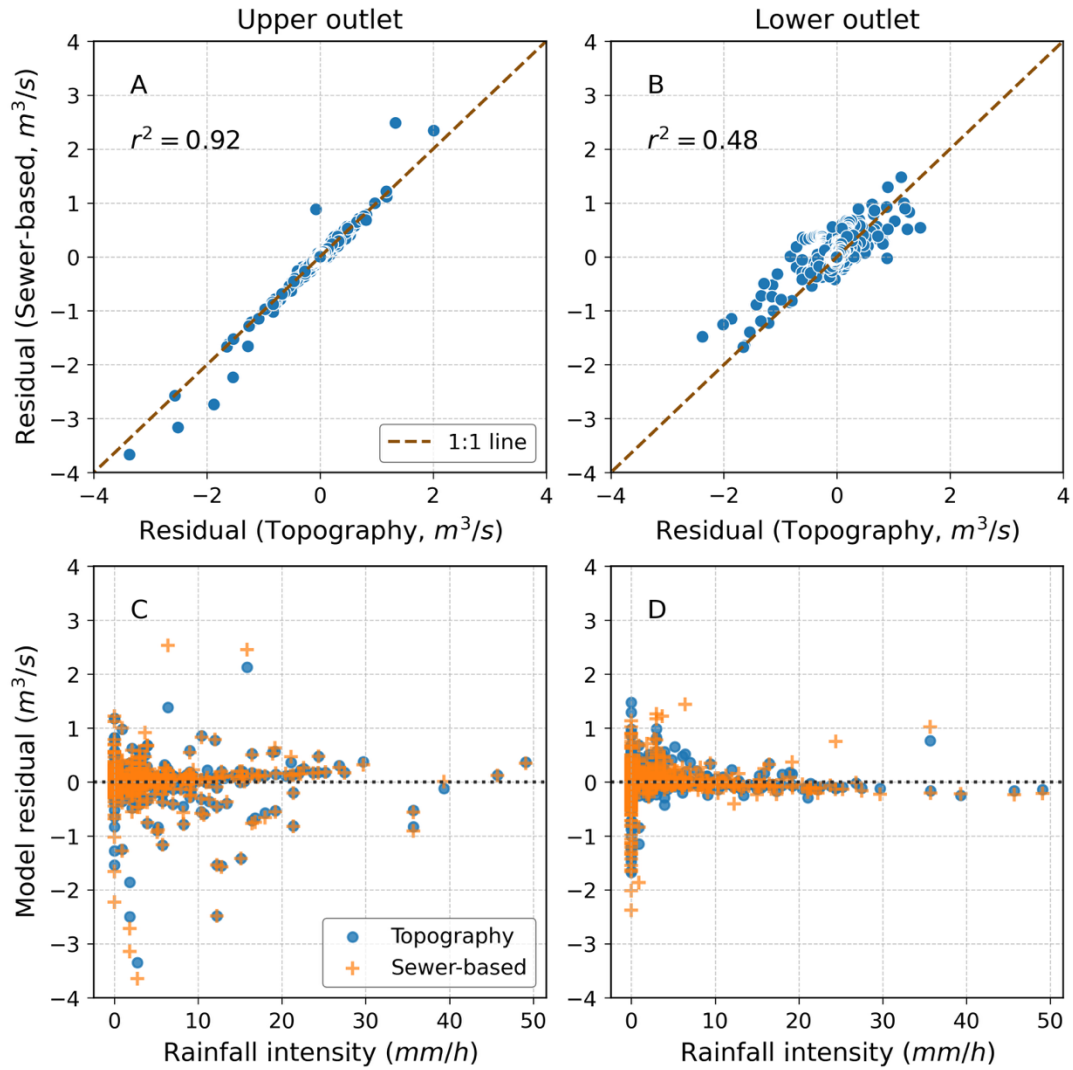
Figure 5. Comparisons of flow residuals (difference between simulated and observed flows)
between the topography- and sewer geometry-based model at the (A) upper outlet and (B) lower
outlet. Models' residuals against rainfall intensity at the (C) upper outlet and (D) lower outlet.

At the two monitoring sites located within the upper and lower watersheds (L1 and L2), although
both models showed decreased performance compared to simulating flows at the watershed
outlets, simulated flows from the topography-based model showed stronger agreement with
observed flows compared with the sewer geometry-based model (Figure 4 and Table S3). The

22

382   mean NSE values during the validation period were 0.82 and 0.83 at L1 and L2, respectively, for

383   the topography-based model compared with 0.66 at L1 and 0.80 at L2, respectively, for the

384   sewer-based model. At location L1, within the upper urban watershed, the lower performance of

385   the sewer geometry-based model may be due to the less representative subcatchment boundaries

386   generated using Thiessen polygons, as discussed in Section 3.2. In contrast, both models yielded

387   similar NSE values at location L2, within the peri-urban area, where the relatively flat terrain and

388   sparsely distributed drainage infrastructure potentially reduced differences caused by the varying

389   drainage boundaries between the two models. However, when comparing runoff volume and

390   peak flow errors (Table S3), the topography-based model still outperformed the sewer geometry-

391   based model at location L2. Overall, these results indicate that while both models can effectively

392   replicate observed flows at the outlets of urban and peri-urban watersheds (with comparable NSE

393   values), the topography-based model was more consistent in simulating observed flows at the

394   monitoring sites located within the watershed. Therefore, to further compare model performance

395   in simulating outlet flows, the next section focuses on evaluating event-based model

396   performance at watershed outlets.

397   **3.2.2 Model performance across events**

398   The total number of individual events ranged from 36 to 42, with a mean of 39 events over the

399   simulation period (2021-2023). The model performance was found to be higher during larger

400   rainfall events (Figure 6). At the upper outlet, the mean NSE values increased from 0.24 to 0.83

401   for the topography-based model and from 0.17 to 0.89 for the sewer geometry-based model as

402   event depth increased from <10 mm to >40 mm. Correspondingly, the absolute mean runoff

403   volume error decreased from 25% to 13% for the topography-based model and from 30% to 19%

404   for the sewer geometry-based model. Further, the absolute mean peak flow error was reduced

405   from 18% to 12% and from 30% to 12%, respectively, as the event depth increased from <10

406   mm to >40 mm. Although the reduction in mean time-to-peak errors was relatively small (~15

407   min) for both models as rainfall depth increased from <10 mm to >40 mm, the range of these

408   errors decreased by more than fivefold. Similar trends in the performance metrics were observed

409   for the lower outlet; however, the performance metrics exhibited greater variability at the lower

410   outlet compared to the upper outlet. These findings further suggest that accurately simulating

411   stormwater flow in peri-urban areas, where natural and urban hydrological processes occur

412   concurrently, is more challenging than in highly urbanized areas. The high sensitivity of model

413   performance to rainfall depth indicates a need for more accurate parameterization of hydrological

414   processes (e.g., infiltration and evapotranspiration), particularly during smaller events (e.g., <10

415   mm), beyond selecting an appropriate watershed-scale discretization approach. Note that it is

416   possible that the overall observed influence of rainfall depth on model performance may be

417   biased by the uneven distribution of events across rainfall depth categories (e.g., 61 events with

418   rainfall depth <10 mm compared with 9 events with depth >30 mm). A more robust evaluation of

419   model performance will require additional rainfall-runoff data to enable more reliable

420   comparisons between the rainfall depth categorizes.

421
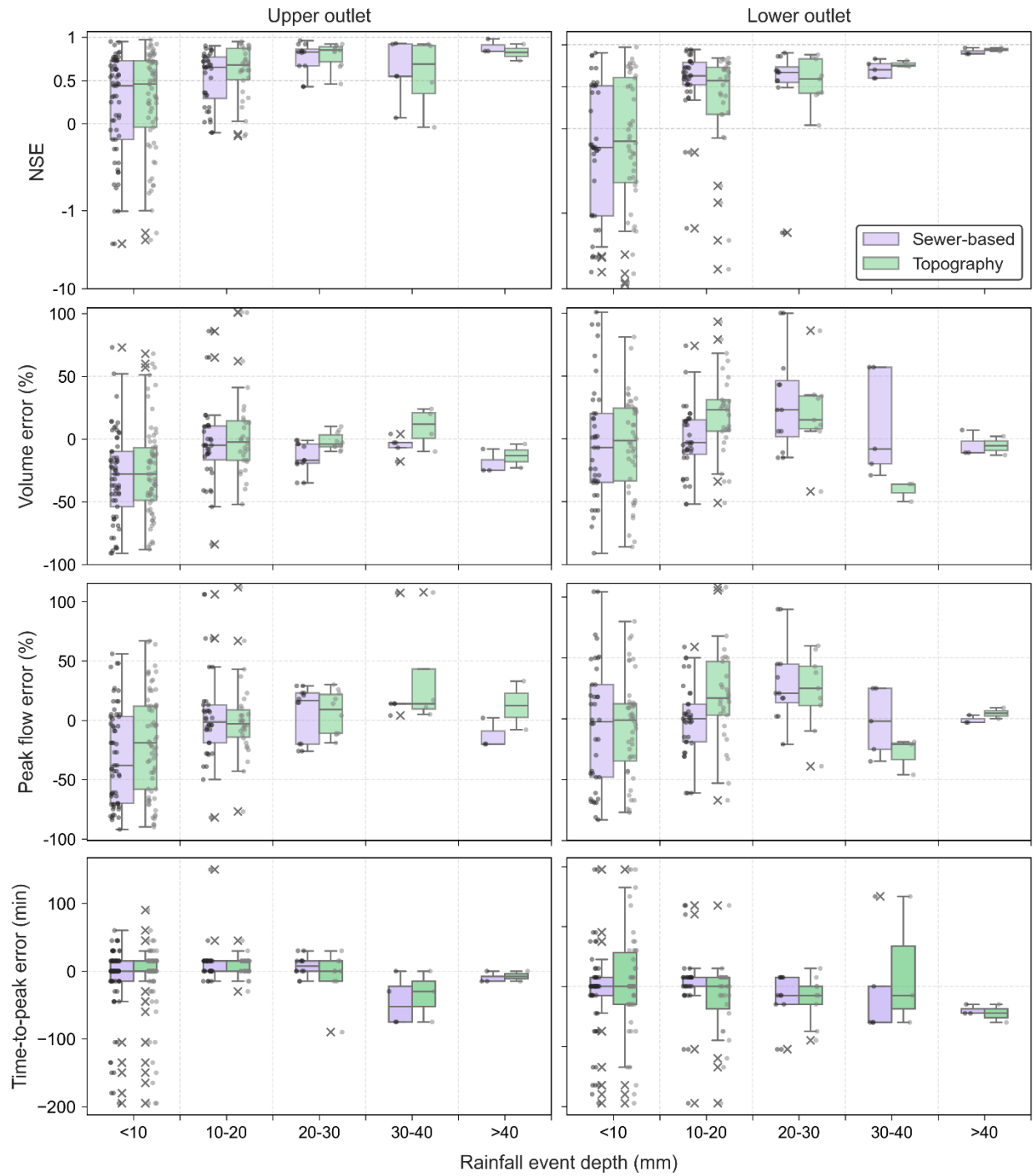
Figure 6. Comparison of NSE values, runoff volume errors (%), peak flow errors (%), and time-to-peak error (min) between the topography-based and sewer-based models for individual events.

424   Comparison between events is presented in five event depth classes: < 10mm, 10-20mm, 20-

425   30mm, 30-40mm, and >40mm. Gray dots indicate the performance of individual events. For

426   readability, NSE values between -1 and 1 are presented on a linear scale, while values outside

427   this range are shown on a log scale.

428   The effects of rainfall depth, discretization approach, and watershed land use characteristics on

429   model performance were further assessed using a linear fixed-effects model (Table 1). Results

430   show the linear fixed-effects model significantly explained the variance in NSE, peak error, and

431   volume error (all $p < 0.001$; Table S4), whereas it did not significantly explain the variance in

432   time-to-peak error ($p = 0.21$). Across all performance metrics evaluated, land use characteristics

433   were a statistically significant predictor of model performance. Note that the lower watershed

434   outlet and sewer geometry-based model were designated as the control group (zero values), so

435   the regression coefficients provided in Table 1 represent differences relative to this baseline.

436   Model performance at the upper urban watershed outlet was significantly better than at the lower

437   outlet, with mean runoff volume and peak flow errors 0.1 and 0.2 lower, respectively, and a

438   mean NSE value that was 0.5 higher (Table 1). Rainfall depth was also a strong predictor. For

439   every additional 1 mm of rainfall, the model indicates that the NSE value is expected to increase

440   by 0.02 with all other variables constant. Similar improvements with increasing rainfall depth

441   were observed in volume error (0.4% lower for additional 1 mm of rainfall) and peak error (0.7%

442   lower). However, discretization approach had no significant effect on any performance metric

443   despite the topography-based model showing slightly better performance (e.g., higher NSE

444   values) compared to the sewer geometry-based model at the upper outlet in the continuous

445   simulations (Figure 4). These results suggest that performance of the model at watershed outlets

446   is most influenced by land use characteristics (urban or peri-urban) and rainfall depth, with

447　limited sensitivity to the watershed discretization approach used. In other words, for outlet flow

448　simulations, the influence of spatial discretization could be mitigated through model calibration

449　to achieve an overall water balance across the entire watershed. This was demonstrated in

450　Section 3.2, where the sewer-geometry-based model exhibited weaker relationships between

451　parameters and hydrological outputs, yet was able to replicate the observed outlet flows.

452　Consequently, the effects of spatial discretization are more apparent in simulating flows within

453　the watershed (as shown in Figure 4 and Table S3). That said, despite its reduced accuracy in

454　locations within the watershed, the sewer geometry-based model still generated acceptable

455　results (all NSE values > 0.5). Overall, linear fixed-effects model further indicates that simpler

456　delineation methods, such as the sewer geometry-based approach, may be an acceptable way to

457　reduce model complexity without significantly compromising simulation accuracy at the outlet.

458　Finally, although this study was conducted for a relatively small mixed urban and peri-urban

459　watershed (~580 ha), it is expected that the findings can be extended to larger watersheds (on the

460　order of thousands of hectares), where the system can be divided into multiple subwatersheds

461　based on outlet configurations and drainage characteristics. However, when aggregating results

462　across subwatersheds, differences in model performance may become more apparent, as

463　simulation variability between the two models may propagate and cumulate from smaller to

464　larger scales. Therefore, future work is needed to evaluate the scalability of both approaches in

465　much larger and more complex watershed settings.

466　**Table 1.** Results of the fixed effects model for the four performance metrics (NSE, peak flow

467　error, volume error, and time-to-peak error). The model includes rainfall depth, discretization

468　approach, and watershed land use characteristics as possible explanatory variables. Values are

469   reported as estimated coefficients when the p-value is <0.05. A sign of "-" indicates a coefficient

470   is not statistically significant (p> 0.05), and thus is not reported.

	NSE	Peak flow error	Time-to-peak error	Volume error
Intercept	-0.3	-0.1	-20.8	-
Land use characteristics	0.5	-0.1	21.7	-0.2
Discretization approach	-	-	-	-
Rainfall depth	0.02	0.007	-	0.004

471   **3.3 Implication and trade-offs**

472   While the models built using the sewer-based and topography-based discretization approaches

473   were both able to simulate well observed flows at the upper and lower watershed outlets, the

474   performance of the models varied in simulating flows at locations within the watershed, and in

475   hydrological representation, and error structure. Key differences between the two approaches are

476   outlined in Table 2. The topography-based model showed a strong relationship between physical

477   parameters and hydrological responses, particularly in the urban watershed with a higher density

478   of drainage infrastructure than in the peri-urban watershed. This suggests the parameter values

479   produced by the topography-based model more likely to reflect underlying hydrological

480   processes. This hydrological interpretability is especially important when simulating surface

481   flooding or assessing the impacts of land use changes or stormwater management scenarios (e.g.,

482   green infrastructure placement). However, topography-based discretization requires high-

483   resolution DEM data and spatial data processing expertise, including integration of DEM with

484   sewer infrastructure or potential further DEM preprocessing (e.g., burning). This increases the

485   complexity of delineating subcatchments and may not be suitable for areas that lack high-

486   resolution spatial data.

487   **Table 2.** Key differences between topography-based and sewer geometry-based discretization

488   approaches.

Aspect	Topography-Based Approach	Sewer Geometry-Based Approach
Stormwater flow prediction at the outlet	High accuracy	Moderate to high accuracy
Simulation of flows within watershed	High accuracy	Adequate overall but less accurate for peak flow
Hydrological representation	Strong correlation between physical parameters and hydrological processes	Relatively weak correlation
Drainage characteristics	Preserves terrain-driven overland flow paths	Tends to generate long, narrow overland flow paths
Rainfall depth impact	High impact on performance	High impact on performance
Implementation complexity	Requiring high resolution DEM, spatial processing, and expert judgment	Low DEM data requirement and single Thiessen polygon generation
Watershed suitability	Both urban and peri-urban watersheds	Better for urban watersheds
Case suitability	Preferred when surface heterogeneity is an important consideration. Better for scenarios of land use, GI design, flooding detection	Effective when primarily interested in outlet flow responses. Better for rapid drainage planning or testing, particularly suitable for areas lacking high-resolution spatial data.

489   In contrast, the sewer geometry-based delineation approach provides a simplified, yet efficient

490   and practical, alternative for watershed discretization. The model developed using this approach

491   produced comparable results to the topography-based model in simulating stormwater flow at

492   watershed outlets (both urban and peri-urban outlets). The simplicity and efficiency of this

493   approach make it suitable for fast, large-scale applications, particularly when sewer datasets are

494   the primary spatial input and the model objective is focused on sewer hydraulics, such as

495   simulating combined sewer overflows (CSOs). However, this simplicity comes at the cost of

496   reduced hydrological interpretability of parameter values and a lower capability to simulate

497   flows at locations within the watershed, particularly in peri-urban areas with mixed drainage

498   systems. Therefore, the choice of discretization strategy should consider the modeling objectives,

499   spatial data availability, and land use and drainage characteristics of the watershed.

4. Conclusion

501   This study evaluated the influence of topography-based and sewer geometry-based discretization

502   strategies on stormwater flow simulations across spatial scales, as well as their effects on model

503   hydrological representation and parameter interpretation in a mixed urban and peri-urban

504   watershed. Simulation results showed that both models were capable of reproducing observed

505   watershed outlet flows, with no statistically significant difference in overall performance (i.e.,

506   NSE, peak flow error, and volume error). However, topography-based discretization produced

507   parameter values with greater hydrological interpretability and yielded more consistent model

508   performance in simulating flows at monitoring sites located within the watershed. Both models

509   showed reduced accuracy during smaller storms (especially < 10mm), indicating that processes

510   that can considerably modify flows during small rainfall depth events (e.g., infiltration and

511   evapotranspiration) may not be well represented in the models. If stormwater management

512   scenarios focus on stormwater flow behaviors during small rainfall events, these hydrological

513   processes should be investigated in future studies. Overall, these findings highlight the

514   significant influence of discretization strategy choice on model robustness across spatial scales

515   and provide practical guidance for urban stormwater modelers and planners, particularly in terms

516   of parameter physical realism and the simulation of flow processes within the watershed.

523   **References**

524   Behrouz, M.S., Zhu, Z., Matott, L.S., Rabideau, A.J., 2020. A new tool for automatic calibration
525   of the Storm Water Management Model (SWMM). J. Hydrol. 581, 124436.
526   https://doi.org/10.1016/j.jhydrol.2019.124436
527   Bibi, T.S., 2022. Modeling urban stormwater management in the town of Dodola based on
528   landuse and climate change using SWMM 5.1. J. Hydrol. Reg. Stud. 44, 101267.
529   https://doi.org/10.1016/j.ejrh.2022.101267
530   Bisht, D.S., Chatterjee, C., Kalakoti, S., Upadhyay, P., Sahoo, M., Panda, A., 2016. Modeling
531   urban floods and drainage using SWMM and MIKE URBAN: a case study. Nat. Hazards
532   84, 749–776. https://doi.org/10.1007/s11069-016-2455-1
533   Braud, I., Fletcher, T.D., Andrieu, H., 2013. Hydrology of peri-urban catchments: Processes and
534   modelling. J. Hydrol. 485, 1–4. https://doi.org/10.1016/j.jhydrol.2013.02.045
535   Dobson, B., Watson-Hill, H., Muhandes, S., Borup, M., Mijic, A., 2022. A Reduced Complexity
536   Model With Graph Partitioning for Rapid Hydraulic Assessment of Sewer Networks.
537   Water Resour. Res. 58, e2021WR030778. https://doi.org/10.1029/2021WR030778
538   Dong, Z., Bain, D.J., Akcakaya, M., Ng, C.A., 2022. Evaluating the Thiessen polygon approach
539   for efficient parameterization of urban stormwater models. Environ. Sci. Pollut. Res. 30,
540   30295–30307. https://doi.org/10.1007/s11356-022-24162-7
541   Dong, Z., Bain, D.J., Buck, J.K., Ng, C., 2024a. Assessment of the long-term hydrological
542   performance of a green roof system in stormwater control. J. Environ. Manage. 370,
543   122831. https://doi.org/10.1016/j.jenvman.2024.122831
544   Dong, Z., Bain, D.J., Paudel, S., Buck, J.K., Ng, C., 2024b. Impact of native vegetation and soil
545   moisture dynamics on evapotranspiration in green roof systems. Sci. Total Environ. 952,
546   175747. https://doi.org/10.1016/j.scitotenv.2024.175747
547   Environment and Climate Change Canada, 2024. Historical Temperature Data.
548   https://climate.weather.gc.ca/historical_data/search_historic_data_e.html
549   Gironás, J., Niemann, J.D., Roesner, L.A., Rodriguez, F., Andrieu, H., 2010. Evaluation of
550   Methods for Representing Urban Terrain in Storm-Water Modeling. J. Hydrol. Eng. 15,
551   1–14. https://doi.org/10.1061/(ASCE)HE.1943-5584.0000142
552   Hopkins, K.G., Bain, D.J., Copeland, E.M., 2014. Reconstruction of a century of landscape
553   modification and hydrologic change in a small urban watershed in Pittsburgh, PA.
554   Landsc. Ecol. 29, 413–424. https://doi.org/10.1007/s10980-013-9972-z
555   Irvine, D.J., Singha, K., Kurylyk, B.L., Briggs, M.A., Sebastian, Y., Tait, D.R., Helton, A.M.,
556   2024. Groundwater-Surface water interactions research: Past trends and future directions.
557   J. Hydrol. 644, 132061. https://doi.org/10.1016/j.jhydrol.2024.132061
558   Jefferson, A.J., Bhaskar, A.S., Hopkins, K.G., Fanelli, R., Avellaneda, P.M., McMillan, S.K.,
559   2017. Stormwater management network effectiveness and implications for urban

560   watershed function: A critical review. Hydrol. Process. 31, 4056–4080.
561   https://doi.org/10.1002/hyp.11347
562 John Fox, 2015. Applied regression analysis and generalized linear models. Sage publications.
563 Krebs, G., Kokkonen, T., Valtanen, M., Setälä, H., Koivusalo, H., 2014. Spatial resolution
564   considerations for urban hydrological modelling. J. Hydrol. 512, 482–497.
565   https://doi.org/10.1016/j.jhydrol.2014.03.013
566 Lee, J.G., Nietch, C.T., Panguluri, S., 2018. Drainage area characterization for evaluating green
567   infrastructure using the Storm Water Management Model. Hydrol. Earth Syst. Sci. 22,
568   2615–2635. https://doi.org/10.5194/hess-22-2615-2018
569 Li, J., Huang, G., Chen, W., 2024. Improvement of City Rainfall Model Subcatchment Structure
570   Based on Urban Hydrology Process. J. Hydrol. Eng. 29, 05024001.
571   https://doi.org/10.1061/JHYEFF.HEENG-6084
572 Macro, K., Matott, L.S., Rabideau, A., Ghodsi, S.H., Zhu, Z., 2019. OSTRICH-SWMM: A new
573   multi-objective optimization tool for green infrastructure planning with SWMM.
574   Environ. Model. Softw. 113, 42–47. https://doi.org/10.1016/j.envsoft.2018.12.004
575 Nash, J.E., Sutcliffe, J.V., 1970. River flow forecasting through conceptual models part I — A
576   discussion of principles. J. Hydrol. 10, 282–290. https://doi.org/10.1016/0022-
577   1694(70)90255-6
578 Ni, T., Zhang, X., Leng, P., Pelling, M., Xu, J., 2025. Comprehensive benefits evaluation of low
579   impact development using scenario analysis and fuzzy decision approach. Sci. Rep. 15,
580   2227. https://doi.org/10.1038/s41598-025-85763-z
581 Niazi, M., Nietch, C., Maghrebi, M., Jackson, N., Bennett, B.R., Tryby, M., Massoudieh, A.,
582   2017. Storm Water Management Model: Performance Review and Gap Analysis. J.
583   Sustain. Water Built Environ. 3, 04017002. https://doi.org/10.1061/JSWBAY.0000817
584 Ontario Ministry of Natural Resources and Forestry, 2019. Authoritative Geospatial Data.
585   https://geohub.lio.gov.on.ca/
586 Perin, R., Trigatti, M., Nicolini, M., Campolo, M., Goi, D., 2020. Automated calibration of the
587   EPA-SWMM model for a small suburban catchment using PEST: a case study. Environ.
588   Monit. Assess. 192, 374. https://doi.org/10.1007/s10661-020-08338-7
589 Qi, M., Lehmann, A., Huang, H., Liu, L., Chen, X., 2025. A SWMM-based evaluation of the
590   impacts of LID and detention basin retrofits on urban flooding. Urban Water J. 22, 51–
591   65. https://doi.org/10.1080/1573062X.2024.2426590
592 Rossman, L.A., Huber, W.C., 2016. Storm Water Management Model Reference Manual
593   Volume I – Hydrology. Washington, DC.
594 Sabrina Jivani, 2024. Modelling seasonal non-point source phosphorus loads from a mixed urban
595   and agricultural land use watershed.
596 Si, Q., Brito, H.C., Alves, P.B.R., Pavao-Zuckerman, M.A., Rufino, I.A.A., Hendricks, M.D.,
597   2024. GIS-based spatial approaches to refining urban catchment delineation that integrate
598   stormwater network infrastructure. Discov. Water 4, 24. https://doi.org/10.1007/s43832-
599   024-00083-z
600 Sokolovskaya, N., Vaughn, C., Jahangiri, H., Smith, V., Wadzuk, B., Ebrahimian, A., Nyquist,
601   J., 2023. Variability of urban drainage area delineation and runoff calculation with
602   topographic resolution and rainfall volume. Water Sci. Technol. 87, 1349–1366.
603   https://doi.org/10.2166/wst.2023.072

604 Vrugt, J.A., Hopmans, J.W., Gao, Y., Rahmati, M., Vanderborght, J., Vereecken, H., 2024. The
605   time validity of Philip's two-term infiltration equation: An elusive theoretical quantity?
606   Vadose Zone J. 23, e20309. https://doi.org/10.1002/vzj2.20309
607 Vyn, D.H., 2023. Effect of land use type and stormwater control measures on non-point source
608   phosphorus concentrations and loads in a cold climate urban subwatershed. Western
609   University, London.
610 Wu, Y., She, D., Xia, J., Zhang, Y., Zou, L., 2024. Evaluation of the number of events' influence
611   on model performance and uncertainty in urban data-scarce areas based on behavioral
612   parameter ranking method. J. Hydrol. 636, 131298.
613   https://doi.org/10.1016/j.jhydrol.2024.131298
614 Zhuang, Q., Li, M., Lu, Z., 2023. Assessing runoff control of low impact development in Hong
615   Kong's dense community with reliable SWMM setup and calibration. J. Environ.
616   Manage. 345, 118599. https://doi.org/10.1016/j.jenvman.2023.118599
617